



LIGO Laboratory / LIGO Scientific Collaboration

LIGO-T040057-00-D

LIGO

4/1/04

Heating Beam Pattern Optical Design
CO2 Laser Thermal Compensation Bench

Michael Smith, David Ottaway, Phil Willems, Cheryl Vorvick, Gerardo Moreno

Distribution of this document:
LIGO Science Collaboration

This is an internal working note
of the LIGO Project.

California Institute of Technology
LIGO Project – MS 18-34
1200 E. California Blvd.
Pasadena, CA 91125
Phone (626) 395-2129
Fax (626) 304-9834
E-mail: info@ligo.caltech.edu

Massachusetts Institute of Technology
LIGO Project – NW17-161
175 Albany St
Cambridge, MA 02139
Phone (617) 253-4824
Fax (617) 253-7014
E-mail: info@ligo.mit.edu

LIGO Hanford Observatory
P.O. Box 1970
Mail Stop S9-02
Richland WA 99352
Phone 509-372-8106
Fax 509-372-8137

LIGO Livingston Observatory
P.O. Box 940
Livingston, LA 70754
Phone 225-686-3100
Fax 225-686-7189

<http://www.ligo.caltech.edu/>

Table of Contents

1	Introduction	4
1.1	Background	4
1.2	Scope	4
1.3	Referenced Documents	4
2	Analysis	5
2.1	Magnification of Projection Telescope	5
2.1.1	Parameter Values	5
2.1.2	Matrix Elements	6
2.1.3	Magnification Ratio of Projection Telescope	7
2.2	Heating Modes	7
2.2.1	Central Heating Mode	8
2.2.2	Annular Heating Mode	12
3	Results	14
3.1	Annular Heating Pattern	14
3.1.1	Magnification of Projection Telescope	14
3.2	Central Heating Pattern	14
4	Conclusions	16

Table of Figures

<i>Figure 1: Thermal compensation system optical bench</i>	5
<i>Figure 2: Beam shaping optical system</i>	7
<i>Figure 3: Airy's disk pattern approximates a Gaussian</i>	10
<i>Figure 4: Diffraction Pattern of Apodized Airy's Disk and Equivalent Gaussian Profile at the Object Plane</i>	12
<i>Figure 5: Projected annular heating pattern at ITM location</i>	14
<i>Figure 6: Projected central heating pattern at ITM location</i>	15
<i>Figure 7: Temperature profile through the center of the projected central heating beam</i>	15

Abstract

The thermal compensation system optical bench projects a central heating spot or an annular heating pattern, illuminated with a CO₂ laser, onto the LIGO interferometer ITM mirror to modify the mode size in the power recycling cavity. The propagation of the beam through the optical system was analyzed using ABCD matrix Gaussian beam propagation methods. Fraunhofer diffraction theory was used to analyze the quasi-Gaussian central heating pattern that was created by spatially filtering the Airy's disc diffraction pattern from a uniformly illuminated aperture.

The projected heating pattern was measured with a FLIR camera, and the actual spot size agreed reasonably well with the calculated design value.

1 Introduction

1.1 Background

The shape and stability of the optical mode in the power recycling cavity of the LIGO interferometer is dependent upon the effective radius of curvature of the high reflectance (HR) mirror of the input test mass (ITM). Since the power recycling cavity includes the substrate of the ITM, any thermally-induced changes in the index of refraction of the ITM substrate due to absorption of the cavity light will change the effective curvature of the ITM and affect the mode structure in the power recycling cavity.

The curvature of the power recycling mirror (PRM) was designed to be optimum at the full, laser operating power of 6W--under the assumption that a known amount of absorption would occur in the beam splitter (BS) and in the ITM mirrors, causing a desirable amount of thermal lensing in the BS and ITM substrates.

The present LIGO interferometers at LHO and LLO are not operating at the maximum power level, and the mirror substrates exhibit different bulk absorptivity than was anticipated. As a result of too much or not enough thermal lensing, the mode structure in the power recycling cavity is often unstable at lower power levels and is generally significantly mismatched with the arm cavity mode size, which causes a reduction in side-band power and optical gain at the antisymmetric port.

One approach for changing the power recycling cavity mode size and structure is to heat the ITM with a projected heating pattern from an external CO₂ laser heat projector (TCS). The preferred heating pattern is either a central Gaussian heating spot, or an annular heating pattern depending upon whether the center of the ITM is being under-heated or overheated by the absorbed cavity light.

1.2 Scope

The purpose of this technical note is to describe the analytical approach that was used for designing the optical system that produces the central and annular heating patterns in the Thermal Compensation System (TCS). Experimental heating profiles that were obtained with the installed TCS at LHO are compared with the design calculations.

1.3 Referenced Documents

Thermal Compensation Installation at LHO, G040172-00-Z, D. Ottaway, K. Mason, S. Ballmer, M. Smith, P. Willems, C. Vorvick, G. Morreno, D. Sigg.

Introduction to Optics, 2nd Ed., F.L. Pedrotti, L.S. Pedrotti (New Jersey: Prentice Hall, 1993)

2 Analysis

A schematic drawing of the thermal compensation system optical bench is shown in Figure 1. The CO2 laser beam from the AOM passes through the beam shaping optical system and the heating pattern is focused onto the ITM with the projection telescope consisting of lenses L3, L4, and parabolic mirror M6.

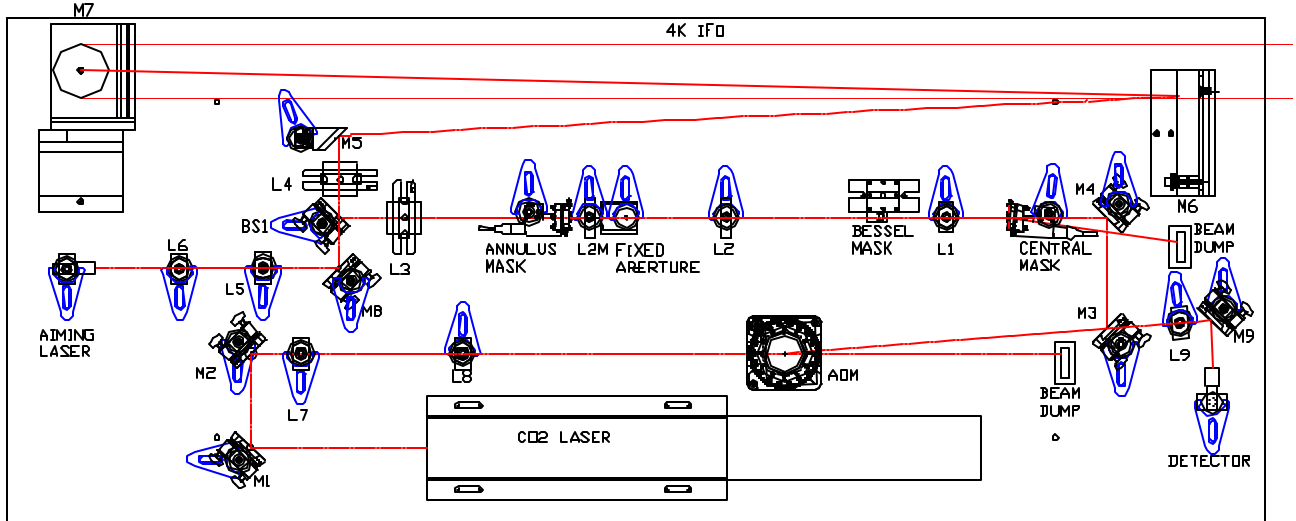


Figure 1: Thermal compensation system optical bench

2.1 Magnification of Projection Telescope

The magnification of the projection telescope portion of the TCS will be calculated using the ABCD matrix Gaussian beam propagation method.

2.1.1 Parameter Values

The following values were used; all length dimensions are given in millimeters:

Focal length of L3	190.5
Distance from L3 to L4	126.1
Focal length of L4	127
Distance from L4 to telescope mirror	

$$l_4(\Delta_f) := f_{L4} + \frac{-R_{20}}{2} + \Delta_f$$

Defocus of telescope	Δ_f	
Radius of telescope mirror		1829

Distance from telescope mirror to lower periscope mirror	1329
Distance from lower periscope mirror to viewport	2000
Distance from viewport to ITM	34000

2.1.2 Matrix Elements

The various matrix elements for the optical path from the annular mask at the object plane to the ITM mirror are shown below:

translation from annular mask to L3	$M3 := \begin{pmatrix} 1 & l_{L3} \\ 0 & 1 \end{pmatrix}$
lens3	$ML3 := \begin{pmatrix} 1 & 0 \\ \frac{1}{-f_{L3}} & 1 \end{pmatrix}$
translation L3 to L4	$M4(\Delta f) := \begin{pmatrix} 1 & l_{L4}(\Delta f) \\ 0 & 1 \end{pmatrix}$
lens4	$ML4 := \begin{pmatrix} 1 & 0 \\ \frac{1}{-f_{L4}} & 1 \end{pmatrix}$
translation L4 to telescope mirror	$Mt(\Delta f) := \begin{pmatrix} 1 & l_4(\Delta f) \\ 0 & 1 \end{pmatrix}$
telescope mirror	$MRt := \begin{pmatrix} 1 & 0 \\ \frac{2}{R_{20}} & 1 \end{pmatrix}$
translation telescope mirror to lower periscope mirror	$Mtmlpm := \begin{pmatrix} 1 & l_{telperim} \\ 0 & 1 \end{pmatrix}$
translation lower periscope mirror to viewport	$Mlpmvp := \begin{pmatrix} 1 & l_{pmpvp} \\ 0 & 1 \end{pmatrix}$
translation from viewport to ITM	$Mitm := \begin{pmatrix} 1 & l_{itm} \\ 0 & 1 \end{pmatrix}$

The total system matrix from the object plane to the ITM is given by

$$M_{itm}(\Delta_f) := M_{itm} \cdot M_{lpmvp} \cdot M_{tmlpm} \cdot MRt \cdot Mt(\Delta_f) \cdot ML4 \cdot M4(\Delta_f) \cdot ML3 \cdot M3$$

$$M_{itm}(\Delta_f) = \begin{pmatrix} 26.549 & -0.079 \\ 9.277 \times 10^{-4} & 0.038 \end{pmatrix}$$

2.1.3 Magnification Ratio of Projection Telescope

In the geometric optics approximation, the projected height h_{itm} at the ITM mirror of an object of height h_1 at the object plane can be calculated from a linear combination of the matrix elements.

$$h_{itm}(\Delta_f) := M_{itm}(\Delta_f)_{0,0} \cdot h_1 + M_{itm}(\Delta_f)_{0,1} \cdot \alpha_1$$

where, h_1 and α_1 are the object height and ray angle at the object plane.

When the telescope is properly focused, the 0,1 element of the matrix will be negligibly smaller than the 0,0 element.

$$\Delta_f := 22.96 \quad \frac{M_{itm}(\Delta_f)_{0,1}}{M_{itm}(\Delta_f)_{0,0}} = -2.975 \times 10^{-3}$$

The magnification ratio is the same for any arbitrary input object height:

$$m := \frac{h_{itm}(\Delta_f)}{h_1} \quad m := M_{itm}(\Delta_f)_{0,0} \quad m = 26.549$$

2.2 Heating Modes

The optical layout of the beam shaping optical system is shown in Figure 2. It consists of a central aperture, which can be inserted or removed from the optical path; lens L1; a fixed Bessel aperture; lens L2; and an annular mask that can be inserted or removed from the optical path.

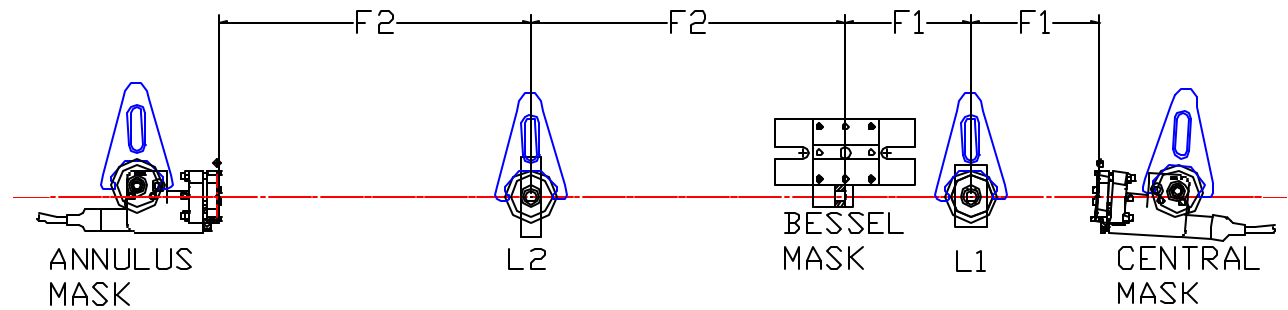


Figure 2: Beam shaping optical system

The physical parameters of the optical system are listed below; dimensions are in millimeters:

Laser wavelength	$10.6 \cdot 10^{-3}$
Focal length of L1	76.2
Focal length of L2	190.5
Central mask diameter	1.651
CO2 waist radius at central mask	2.895
Bessel mask diameter	1.191

There are two modes of operation: central heating and annular heating.

2.2.1 Central Heating Mode

A quasi-Gaussian central heating spot is produced by illuminating the central mask hole of diameter D , located at the front focal plane of L1, a distance F_1 in front of lens L1 with an oversize Gaussian beam of radius w_{cm} from the AOM. L1 forms the Fraunhofer diffraction pattern of the central mask hole at the back focal plane of L1 (called the Bessel plane), which with a uniform illumination of the central mask is the familiar Airy's disk pattern. An apodizing aperture of diameter d , equal to the diameter of the 1st null of the Airy's disk pattern and located at the Bessel plane, acts as a spatial filter that passes only the central lobe of the Airy's disk pattern.

2.2.1.1 Uniform Illumination of Central Mask

The Fraunhofer diffraction amplitude function in the Bessel plane of the illuminated mask is proportional to the complex Fourier transform of the mask illumination function constrained within the diameter of the central mask, D . The lower case x, y coordinates refer to the central mask plane; the upper case coordinates refer to the Bessel plane.

uniform illumination function $A(x, y) := 1$

Fraunhofer diffraction amplitude function

$$E_{TH}(X, Y) := \int_{-\frac{D}{2}}^{\frac{D}{2}} \int_{-\left[\left(\frac{D}{2}\right)^2 - y^2\right]^{0.5}}^{\left[\left(\frac{D}{2}\right)^2 - y^2\right]^{0.5}} A(x, y) \cdot e^{i \left[x \cdot \left(2 \cdot \pi \cdot \frac{X}{\lambda \cdot F_1} \right) + y \cdot \left(2 \cdot \pi \cdot \frac{Y}{\lambda \cdot F_1} \right) \right]} dx dy$$

For the purpose of comparing various intensity profiles, the amplitude function is normalized by dividing by the on-axis peak amplitude.

$$\text{normalized amplitude function} \quad E_{\text{NTH}}(X, Y) := \frac{E_{\text{TH}}(X, Y)}{E_{\text{TH}}(0, 0)}$$

2.2.1.2 Gaussian Beam Illumination of Central Mask

The actual illumination of the central mask is not uniform, but has a Gaussian beam shape with an amplitude function given by the following:

$$A(x, y, w_{\text{cm}}) := e^{-\frac{(x^2 + y^2)}{w_{\text{cm}}^2}}$$

Figure 3 compares the Fraunhofer intensity patterns obtained at the Bessel plane from a uniform illumination of the central mask hole with various Gaussian illumination functions of differing beam waists: 2.895 mm, 1.0 mm, and 0.5 mm. It can be seen that the $w_{\text{cm}} = 2.895$ beam waist from the divergent AOM beam is uniform enough to produce almost exactly the same Airy's disk intensity pattern as a perfectly uniform illumination would produce. To simplify the ensuing analysis, we will assume that the diffraction pattern at the Bessel plane can be described by the Airy's disk amplitude function.

An equivalent Gaussian beam intensity pattern is also shown in Figure 3, which will produce the same diffraction intensity at the object plane, measured at the 50% intensity diameter, as the apodized Airy's disk pattern—see Figure 4.

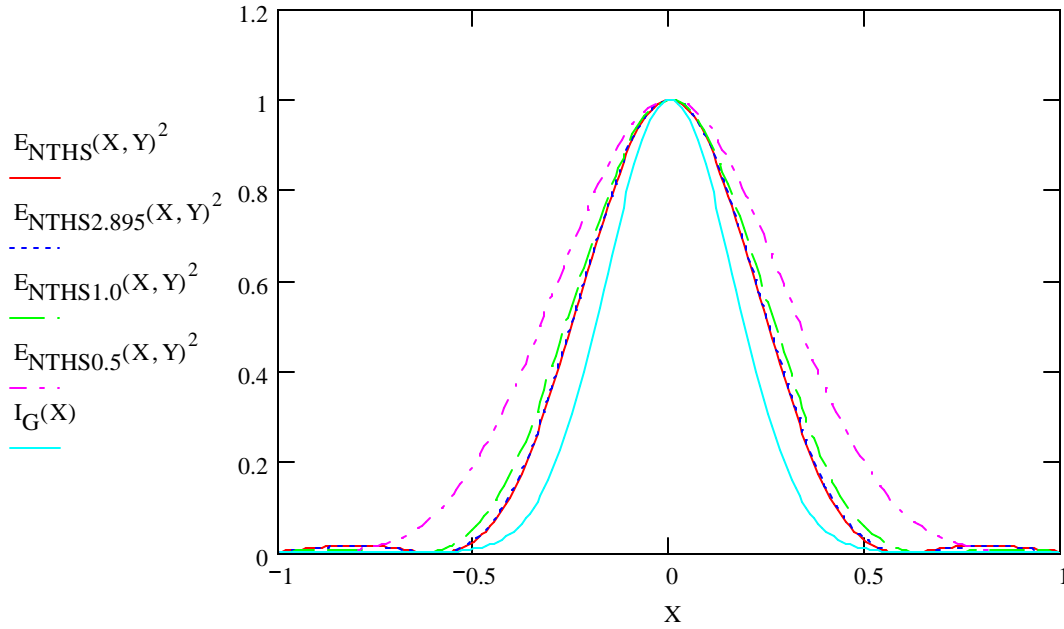


Figure 3: Airy's disk pattern approximates a Gaussian

2.2.1.3 Quasi-Gaussian Diffraction Pattern of the Apodized Airy's Disk

We can produce a quasi-Gaussian intensity pattern at the back focal plane of L2 by clipping the Airy's disk amplitude function with an apodizing aperture having a diameter equal to the first null of the Bessel function, which only allows the central lobe to pass through.

The Airy's disk amplitude function in the Bessel plane is given by

$$A(x, y) := 2 \cdot \frac{J_1(\gamma(x, y))}{\gamma(x, y)}$$

The Bessel function argument is given by

$$\gamma(x, y) := \frac{\pi \cdot D \cdot (x^2 + y^2)^{0.5}}{\lambda \cdot F_1}$$

where x, y are the coordinates at the Bessel plane, D is the diameter of the hole in the central mask, F_1 is the focal length of L1, λ is the wavelength of the laser beam.

The Fraunhofer diffraction amplitude of the apodized Airy's disk pattern in the object plane is given by the complex Fourier transform of the Airy's disk amplitude function constrained within the diameter of the apodizing aperture, d .

$$E_{TA}(X, Y) := \int_{-\frac{d}{2}}^{\frac{d}{2}} \int_{-\left[\left(\frac{d}{2}\right)^2 - y^2\right]^{0.5}}^{\left[\left(\frac{d}{2}\right)^2 - y^2\right]^{0.5}} A(x, y) \cdot e^{i \left[x \cdot \left(2 \cdot \pi \cdot \frac{X}{\lambda \cdot F_2} \right) + y \cdot \left(2 \cdot \pi \cdot \frac{Y}{\lambda \cdot F_2} \right) \right]} dx dy$$

where x, y are the coordinates in the Bessel plane, X, Y are the coordinates in the object plane, and F_2 is the focal length of L2.

The normalized intensity function for the apodized Airy's disk diffraction is given by

$$I_{TA}(X, Y) := \frac{E_{TA}(X, Y)^2}{E_{TA}(0, 0)^2}$$

Similarly, the Fraunhofer diffraction amplitude of an equivalent Gaussian profile matched to the 50% intensity diameter can be calculated.

The Gaussian amplitude function is given by

$$E_G(x, y) := e^{-\frac{(x^2 + y^2)}{w_0^2}}$$

The Fraunhofer diffraction amplitude of the Gaussian amplitude function is given by

$$E_{TG}(X, Y) := \int_{-20 \cdot w_0}^{20 \cdot w_0} \int_{-(20 \cdot w_0)}^{20 \cdot w_0} E_G(x, y) \cdot e^{i \left[x \cdot \left(2 \cdot \pi \cdot \frac{X}{\lambda \cdot F_2} \right) + y \cdot \left(2 \cdot \pi \cdot \frac{Y}{\lambda \cdot F_2} \right) \right]} dx dy$$

The normalized Gaussian intensity function for the diffracted Gaussian pattern is given by

$$I_{TG}(X, Y) := \frac{E_{TG}(X, Y)^2}{E_{TG}(0, 0)^2}$$

We verified that the finite integration limits yield a reasonably close approximation to the exact value obtained with infinite limits, by comparing the calculated 13.5% intensity beam radius with the theoretical Gaussian spot size given by the following:

$$w_{13.5} := \lambda \cdot \frac{F_2}{\pi \cdot w_0}$$

The intensity patterns of the apodized Airy's disk and the equivalent Gaussian beam in the object plane are compared in Figure 4.

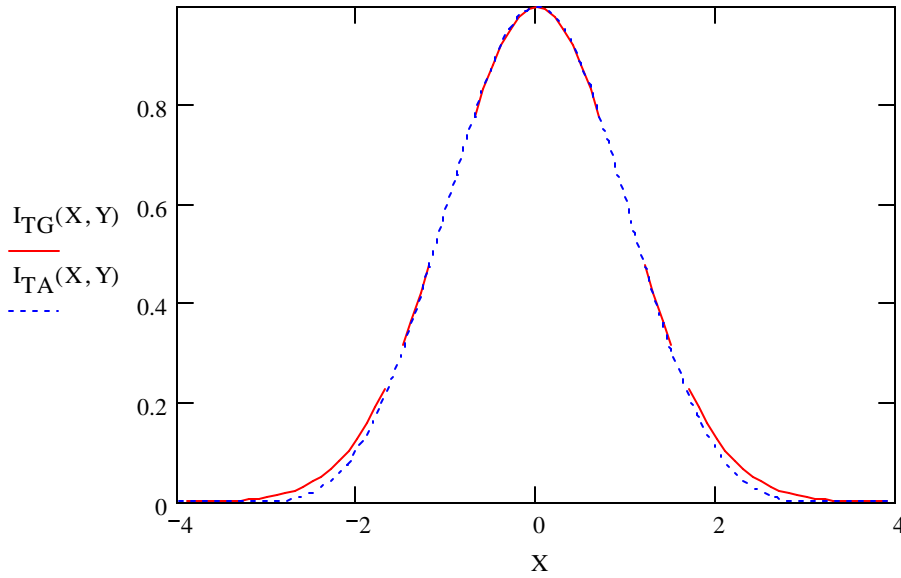


Figure 4: Diffraction Pattern of Apodized Airy's Disk and Equivalent Gaussian Profile at the Object Plane

2.2.1.4 Equivalent Gaussian Beam

We determined empirically that the equivalent Gaussian beam at the Bessel plane has a calculated spot size radius approximately half the radius of the Airy's disk first null.

$$w_0 := 0.546 \cdot \frac{d}{2} \quad w_0 = 0.325$$

The beam waist radius of the equivalent Gaussian beam at the object plane is

$$w = 1.98 \text{ mm.}$$

They both have a 50% intensity diameter in the object plane of

$$2.30 \text{ mm.}$$

2.2.1.5 Central Spot Illumination Pattern at the ITM

Using the calculated magnification ratio of the imaging telescope of 26.5, the 50% intensity diameter of the projected central heating beam on the ITM is calculated to be 61.0 mm.

2.2.2 Annular Heating Mode

To create the annular heating pattern, the central heating mask is removed; the annular mask is inserted at the object plane, and is illuminated by the Gaussian beam.

The waist radius of the illuminating Gaussian beam at the object plane is calculated to be $w = 6.529$ mm.

The dimensions of the annular mask are the following:

inner disk diameter = 3.2 mm

outer disk diameter = 9.6 mm

Using the calculated magnification ratio of the imaging telescope of 26.5, the image size of the annular mask on the ITM is calculated to be:

inner disk diameter = 85 mm

outer disk diameter = 254 mm

3 Results

3.1 Annular Heating Pattern

A FLIR camera image of the annular heating pattern projected onto a paper screen at approximately the same projection distance to the ITM is shown in Figure 5. The horizontal and vertical bars are the image of the spokes that hold the central disk in the center of the outer hole diameter. The diameter of the illuminating Gaussian beam is not large enough to uniformly illuminate the annulus.

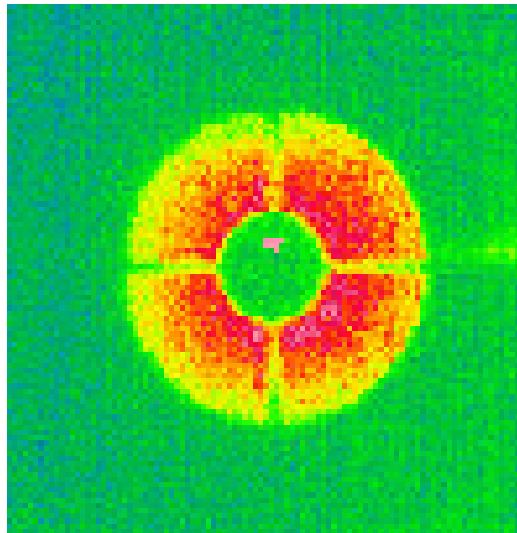


Figure 5: Projected annular heating pattern at ITM location

3.1.1 Measurement of the Magnification of Projection Telescope

The outer ring was measured directly on the projection screen to be approximately 235 mm diameter, and the inner ring was measured to be approximately 82mm. Based on these measurements and the known dimensions of the annular mask, the measured magnification of the projection telescope is approximately 24.9. This is comparable to the calculated value of 26.5

3.2 Central Heating Pattern

A FLIR camera image of the central heating pattern projected onto a paper screen at approximately the same projection distance to the ITM is shown in Figure 6.

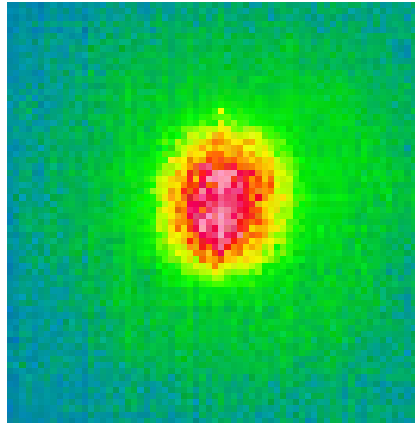


Figure 6: Projected central heating pattern at ITM location

The measured temperature profile from the FLIR photograph, in a cross-section passing through the center of the central heating pattern, is shown in Figure 7.

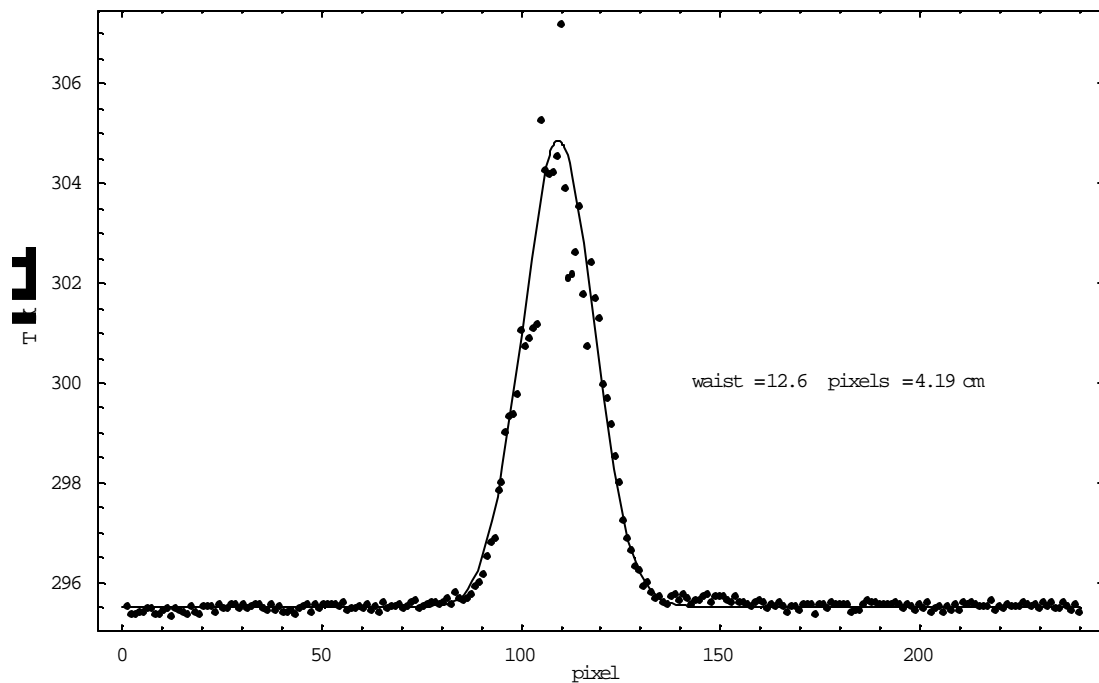


Figure 7: Temperature profile through the center of the projected central heating beam

Assuming that the temperature profile on the paper projection screen is the same as the intensity profile of the heating beam, the projected intensity pattern approximates that of a Gaussian beam with a beam waist radius of 42 mm.

Using the calculated beam waist radius of 1.98 at the object plane, and the measured magnification ratio of 24.9, we calculate the projected central heating beam waist radius to be 49 mm. This is comparable to the measured value of 42 mm.

4 Conclusions

The ABCD Gaussian beam propagation method for analyzing the optical system, and the Fraunhofer diffraction theory used for calculating the diffraction patterns through the mask planes provide an adequate approach for designing the thermal compensation bench optical system.